31 August 1964
WT:bb:401
997-112

MEMORANDUM

To:
From:
Subject: Continuation of Study to Determine Density Variation with Numerical Aperture
CC:

INTRODUCTION

The purpose of this memorandum is to present the results of the continuation of the study of density variation with numerical aperture. This project was initiated by and described in detail in an earlier memorandum.[1]

Specifically, this memo contains the results of diffuse density measurements using the MacBeth densitometer. These results are expressed in terms of Callier's q factor.

EXPERIMENTAL PROCEDURE

The difficulties encountered previously with the MacBeth densitometer were corrected by replacing the defective diffuser with a new pot opal diffuser.[2] The densitometer was then recalibrated using the calibration step wedge and checked with the neutral density glass filters. Agreement between the stated densities of the glass filters and the experimental readings were to within .04 density units, except for the 1.61 filter which was measured as 1.51 on the MacBeth densitometer.

[1] Memorandum, HH:bb:362 (997-112), 31 July 1964

[2] Memorandum, HH:bb:359 (997-112), 7 August 1964

The diffuse densities of the sample step wedges described in Reference 1 were measured using the MacBeth densitometer. The films considered were Eastman Kodak 8401, SO-278, SO-243, SO-105, SO-136 (2 min., 5 min., and 12 min. development times), and commercial Panatomic X.

RESULTS

The following notation will be adopted for the density D pertaining to a certain combination of source numerical aperture x and detector numerical aperture y:

$$D \equiv D(x, y)$$

Continuing with the notation of Reference 1, a generalized Callier's factor is defined as

$$q(x,y)_m \equiv \frac{D(x,y)_m}{D(o,1)_m}$$

In this experiment, $D(x,y)$ refers to the density values obtained from the sample wedges at the given numerical aperture combinations. These results were reported in Reference 1. $D(o,1)$ refers to the diffuse densities measured on the MacBeth densitometer. For these measurements, the illuminating light was collimated making the source numerical aperture approximately .05 and the diffusing pot opal made the detector numerical aperture approximately 1. The subscript m in the formula above indicates that for each value of q, $D(x,y)$ and $D(o,1)$ must be evaluated for the same step of the sample wedges. Hence, for each of the numerical aperture combinations and for each sample film a continuous curve can be drawn.

The usefulness of the q factor is in the prediction of a density $D(x_2, y_2)$ when $D(x_1, y_1)$ is known (see Reference 1, Page 5). Thus:

$$D(x_2, y_2) = \left[\frac{q(x_2, y_2)}{q(x_1, y_1)}\right] D(x_1, y_1)$$

Figures (1) through (7) illustrate how $q(x,y)$ varies with $D(x,y)$ for all the sample film types except SO-105 whose q factor is unity within experimental error. Some of the curves represent more than one numerical aperture combination since the q factors are approximately equal at all steps.

Figures (8) through (14) show how $q(x,y)$ varies with $D(o,1)$ for each of the sample film types. Again q was not plotted for SO-105 since it was approximately unity.

The q vs. D and q vs. $D(o,1)$ curves illustrate the higher values of q corresponding to higher values of granularity (Reference 1, Page 5) for a given aperture combination and the approach of q to unity as D decreases to zero.

Figures (1) through (14) illustrate the non-linear dependence of q on $D(x,y)$ and $D(o,1)$. The solid curves have been drawn to fit the data points. The logarithmic relation between the q factor and density[3] is borne out by Figures (15) through (17) which are plots of $\log_{10} q$ vs. $\log_{10} D(o,1)$. In the case of Panatomic X film, two of the straight lines on the log-log plots were converted to linear scales. These curves are drawn on Figure (8) as dashed lines. These smoothed curves show quite distinctly the effect of the densitometer non-linearities.

It is now possible to find $D(x_2, y_2)$ when $D(x_1, y_1)$ is known by following the procedure given in Reference 1, Page 13.

STAT

[3] James, T.H. and Higgins, G.C., Fundamentals of Photographic Theory, Morgan and Morgan Publishing Co., (1960), Chapter 10.

Fig. (1) - Variation of q with D for Panatomic-X Film.

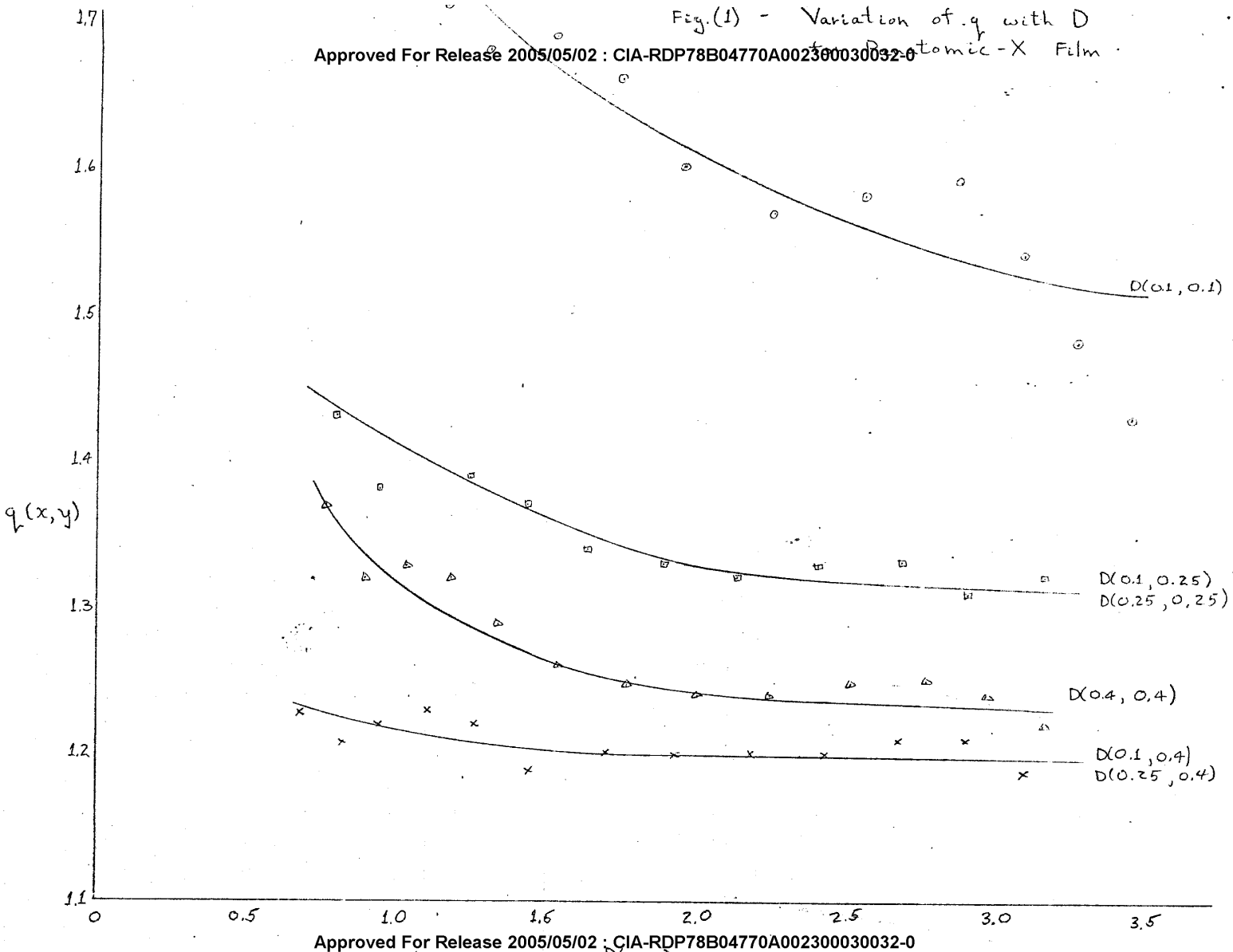

Fig.(2)- Variation of q_r with D for Film Type SO-278

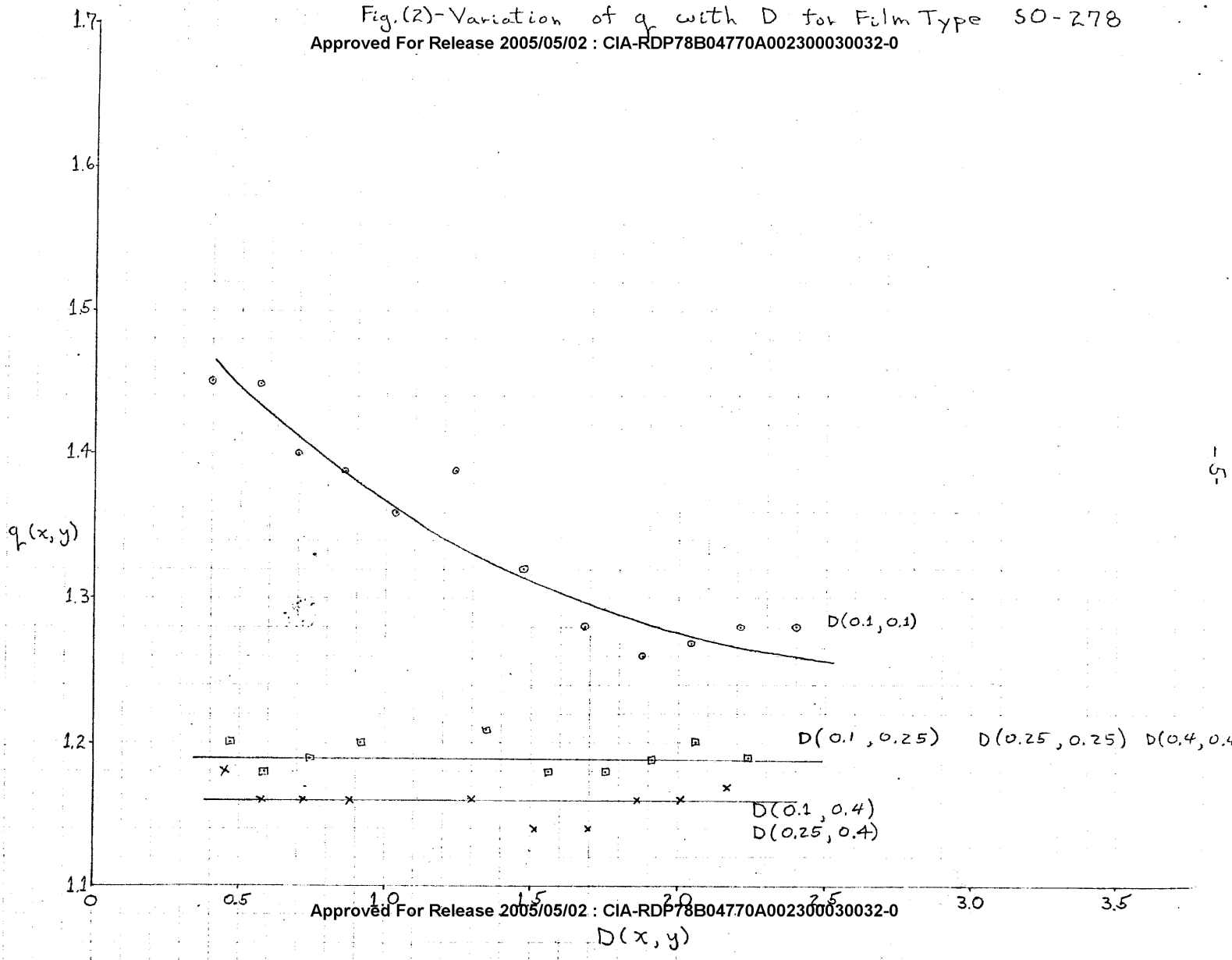

Fig.(3) - Variation of q_r with D for Film Type SO-243

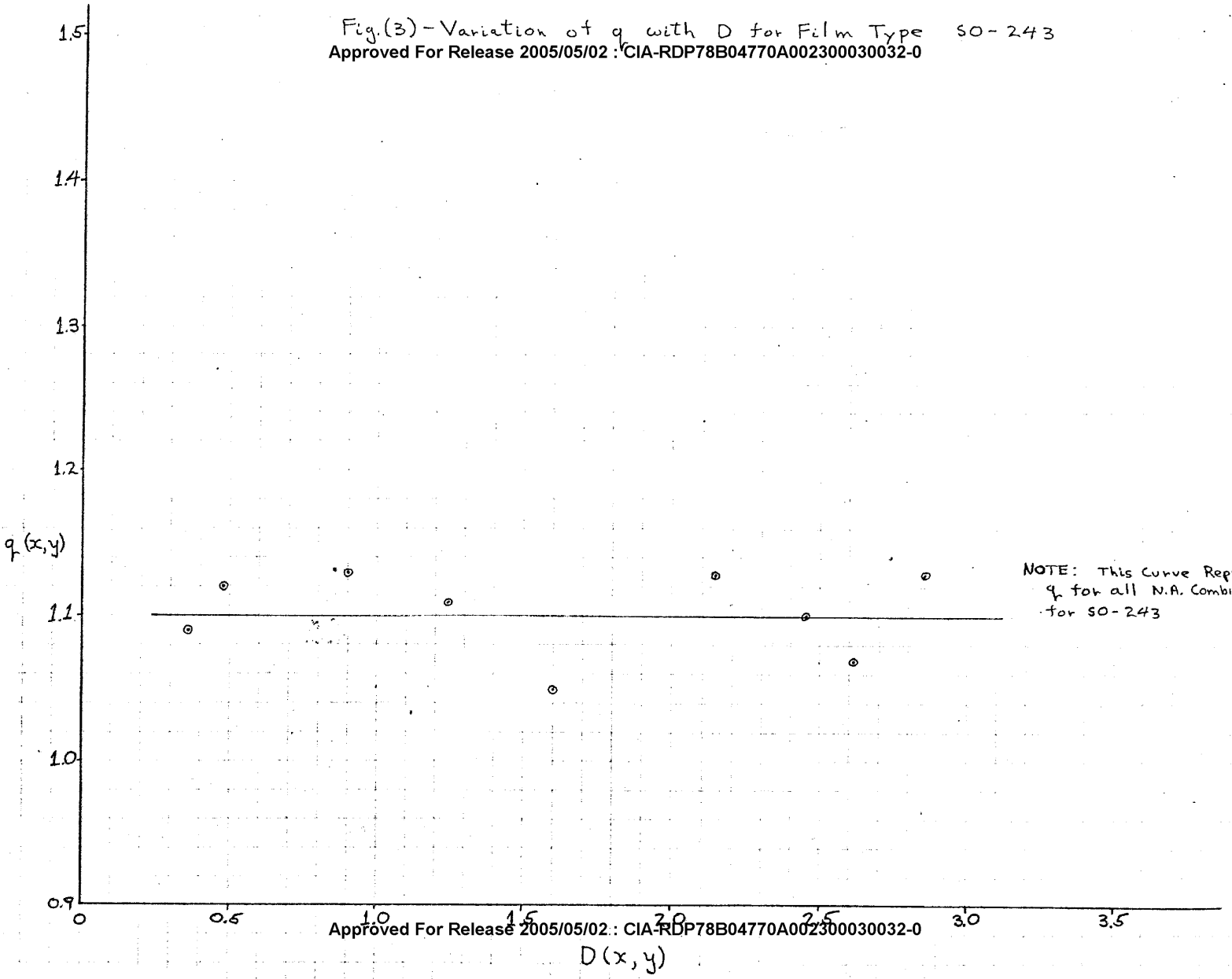

Fig.(4) Variation of q with D
for Failure Time 50 Days (3 Min. Development)

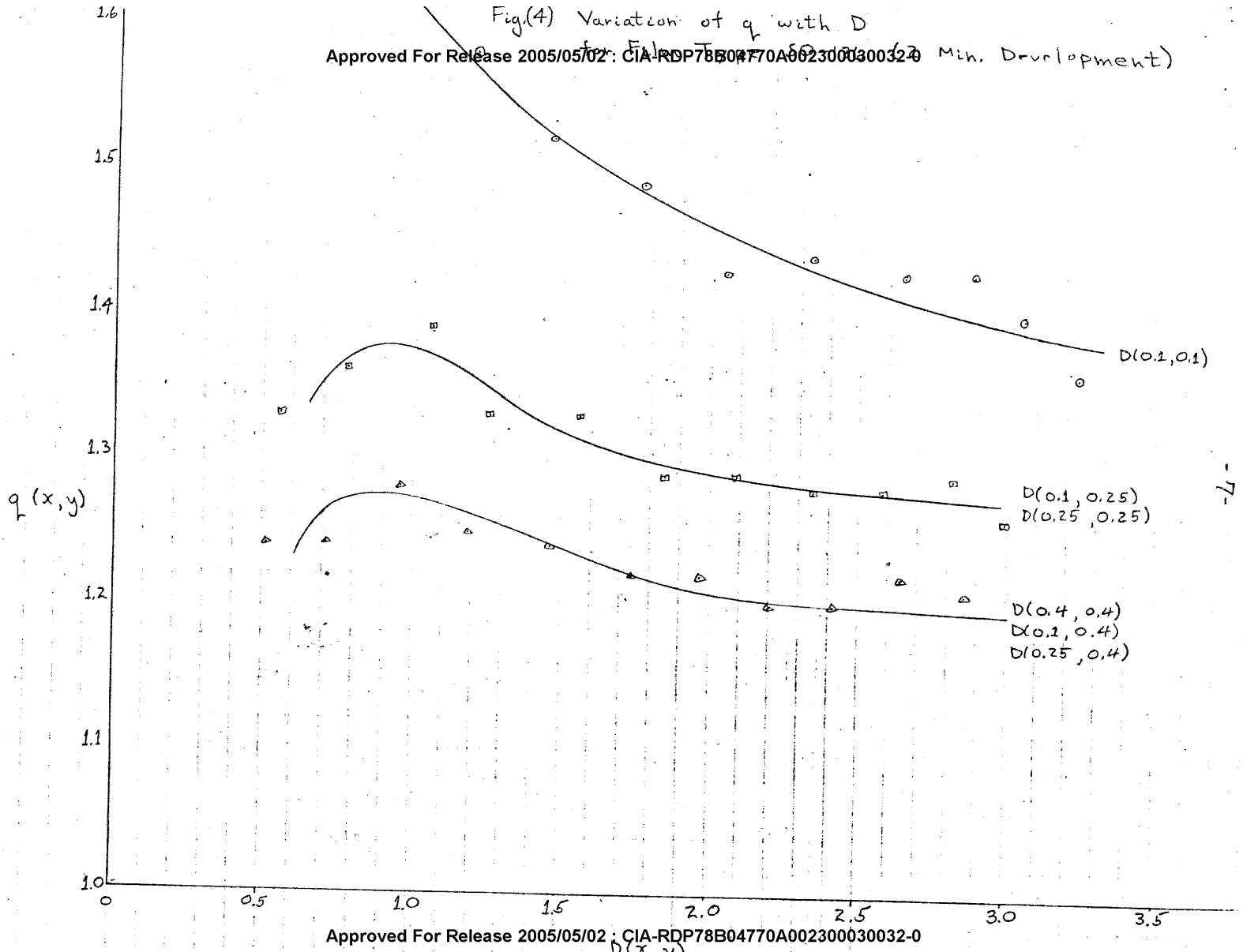

Fig.(5) Variation of γ with D for Film Type SO-136 (5 Min. Development)

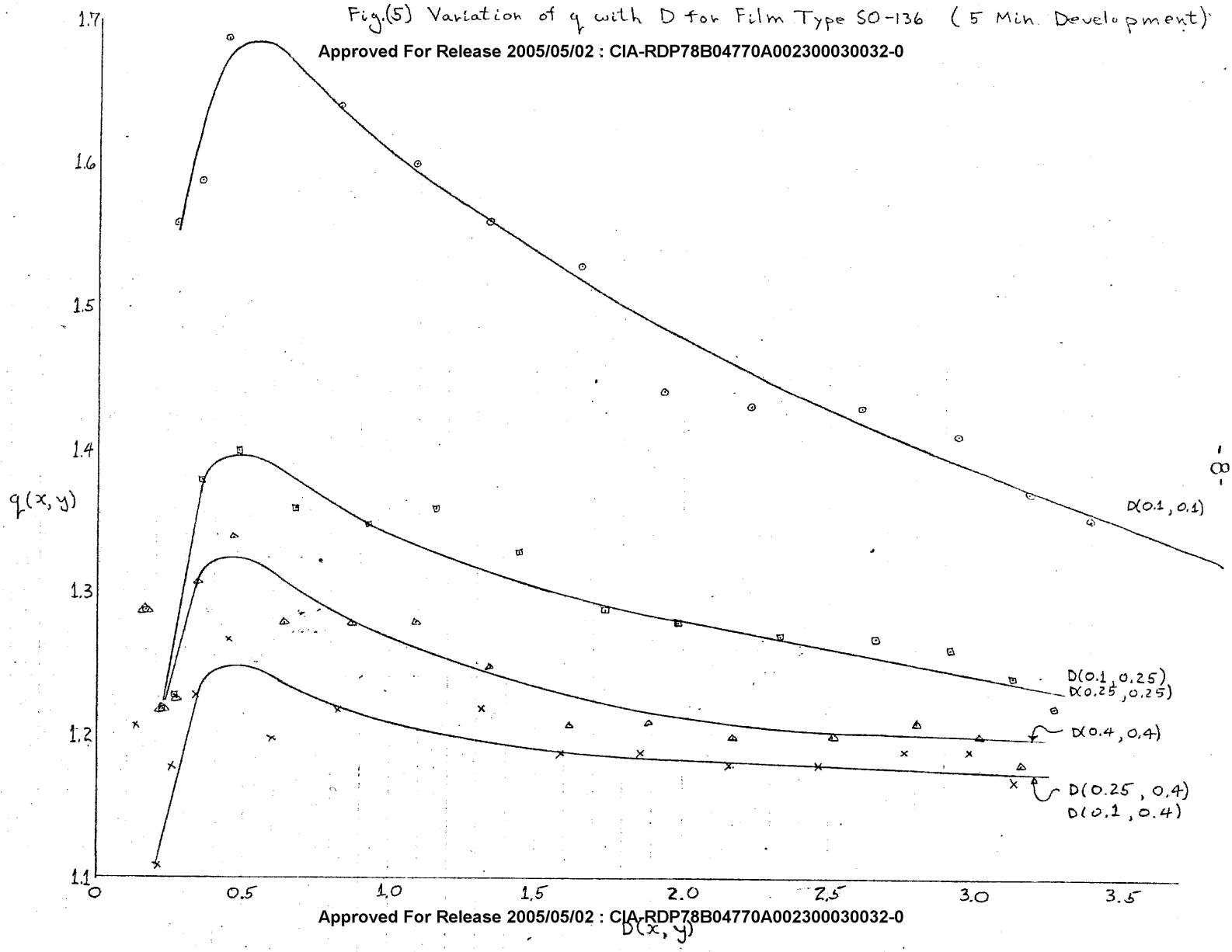

Fig.(6) Variation of q with D for Film Type SO-136 (12 Min. Development)

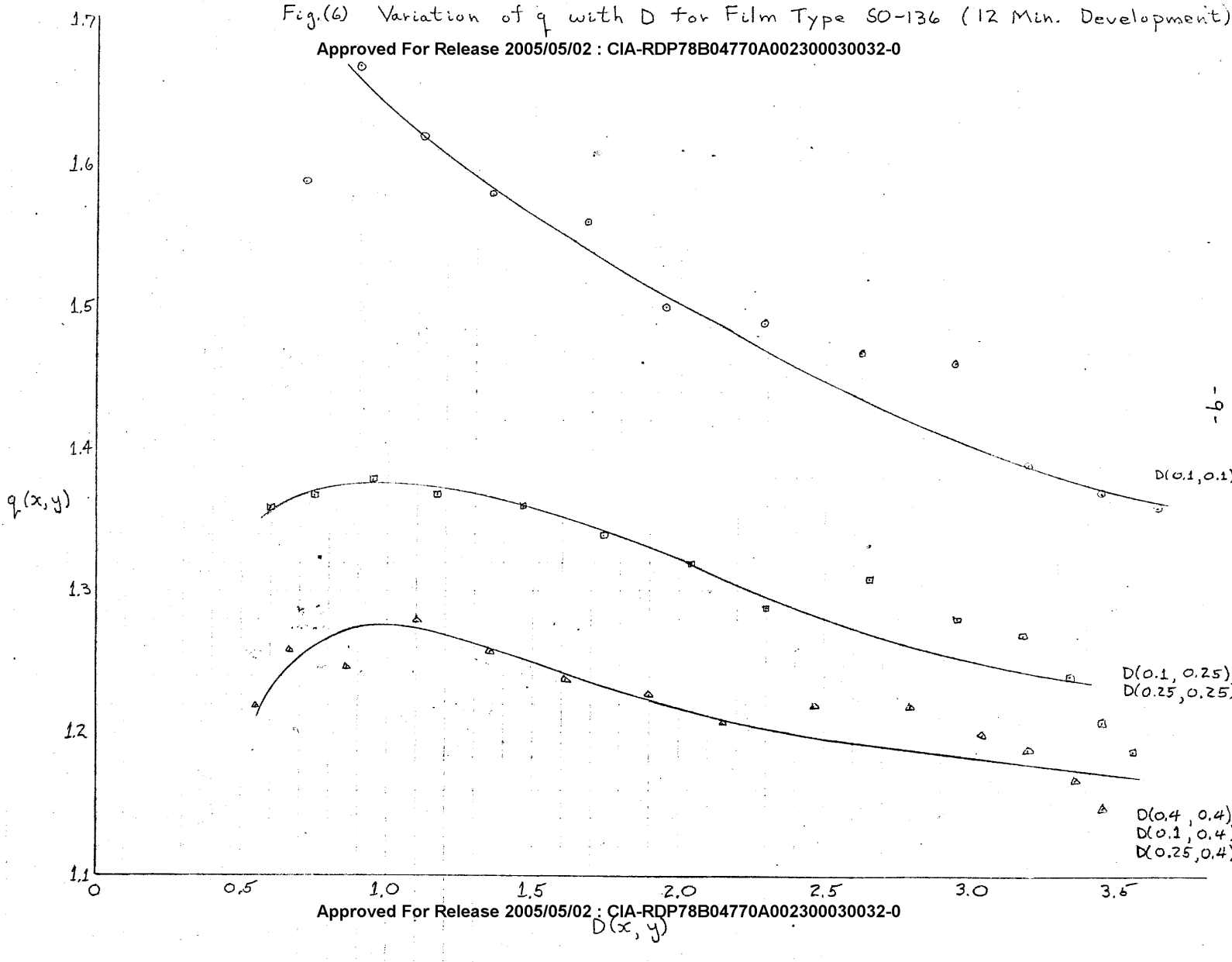

Fig. (4.1) Variation of q with D for Film Type 8401

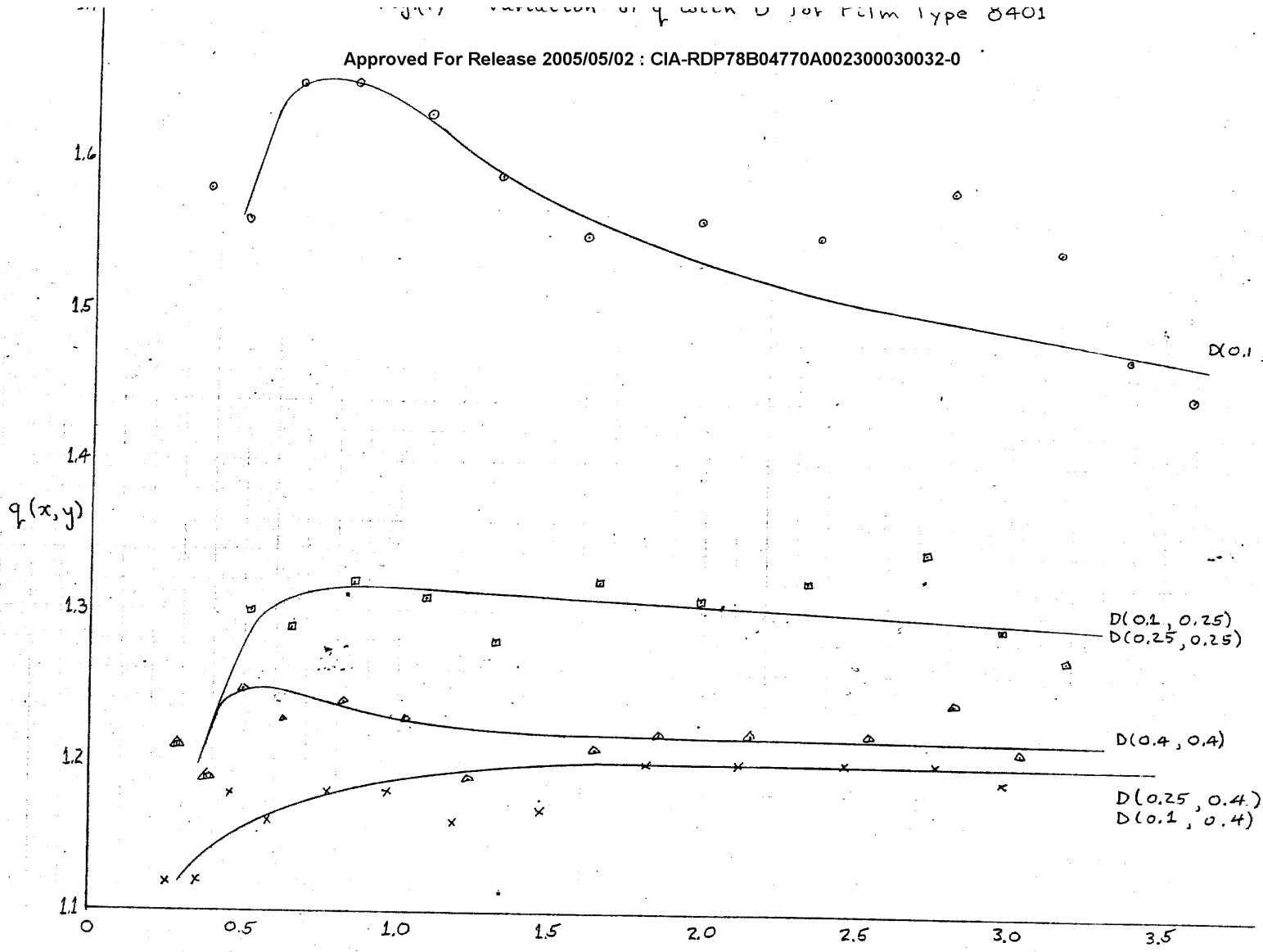

Fig(8) - Variation of q with D(0,1) for Panatomic-X Film.

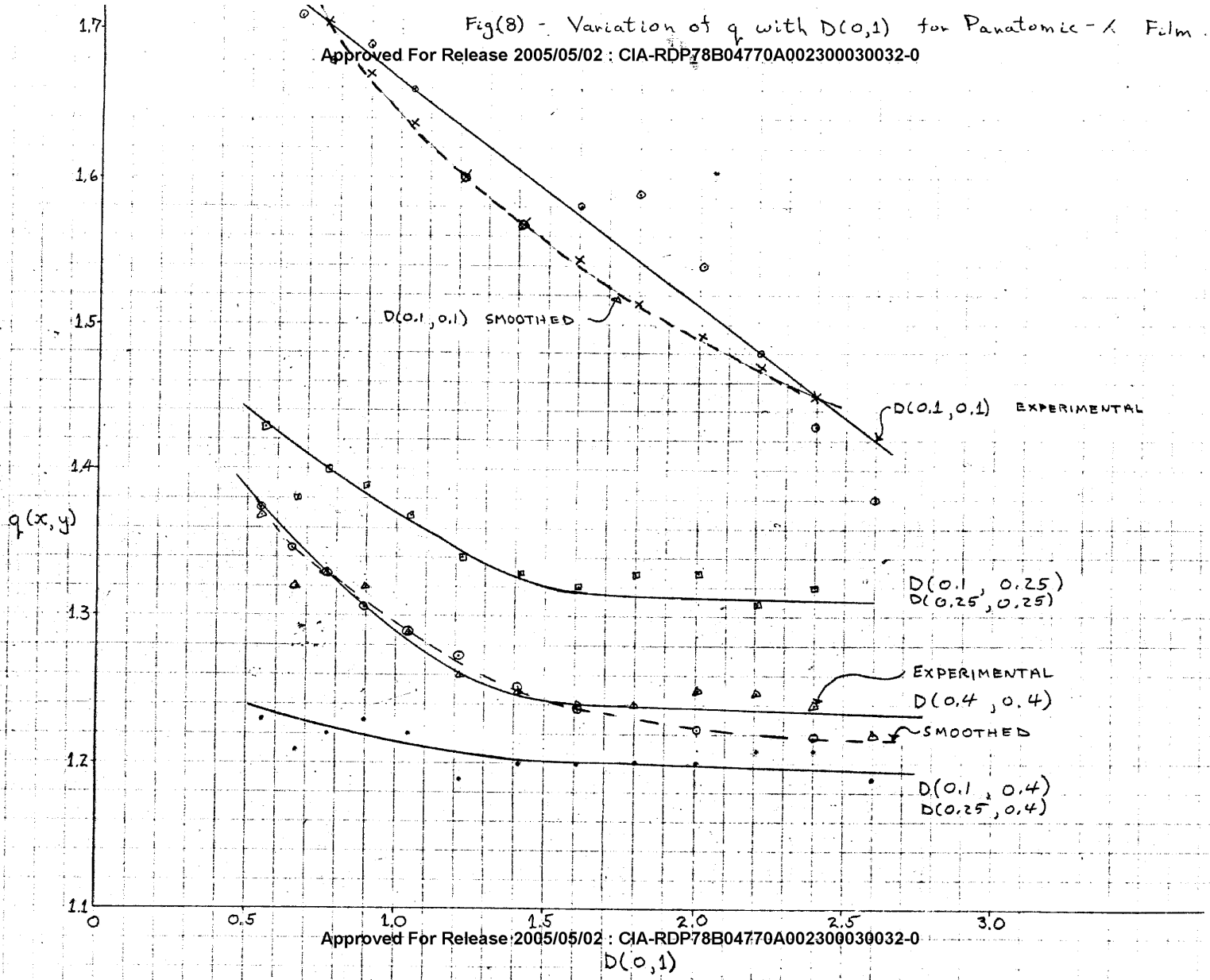

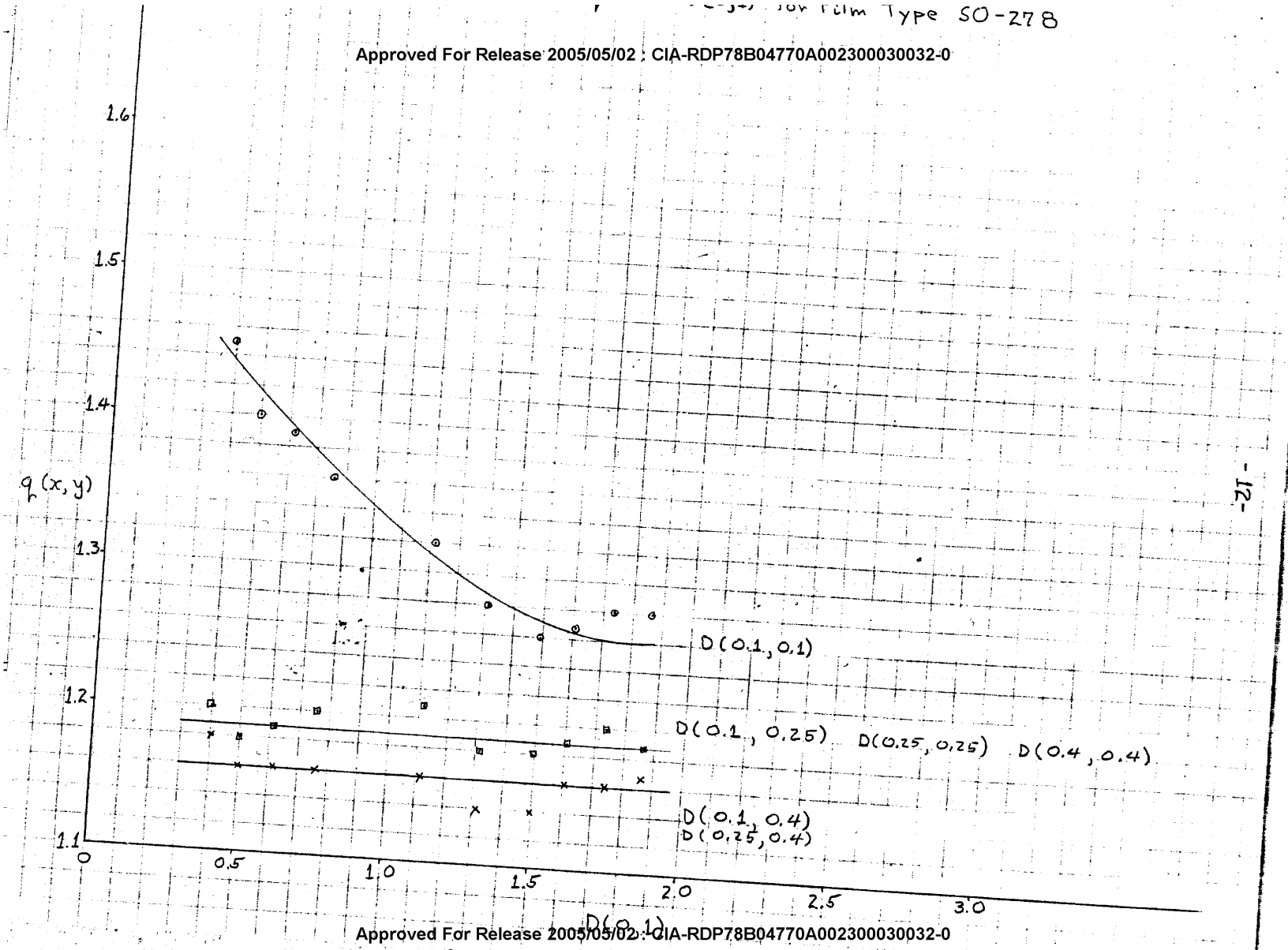

Fig (10) - Variation of q_r with D(o,1) for Film Type SO-243

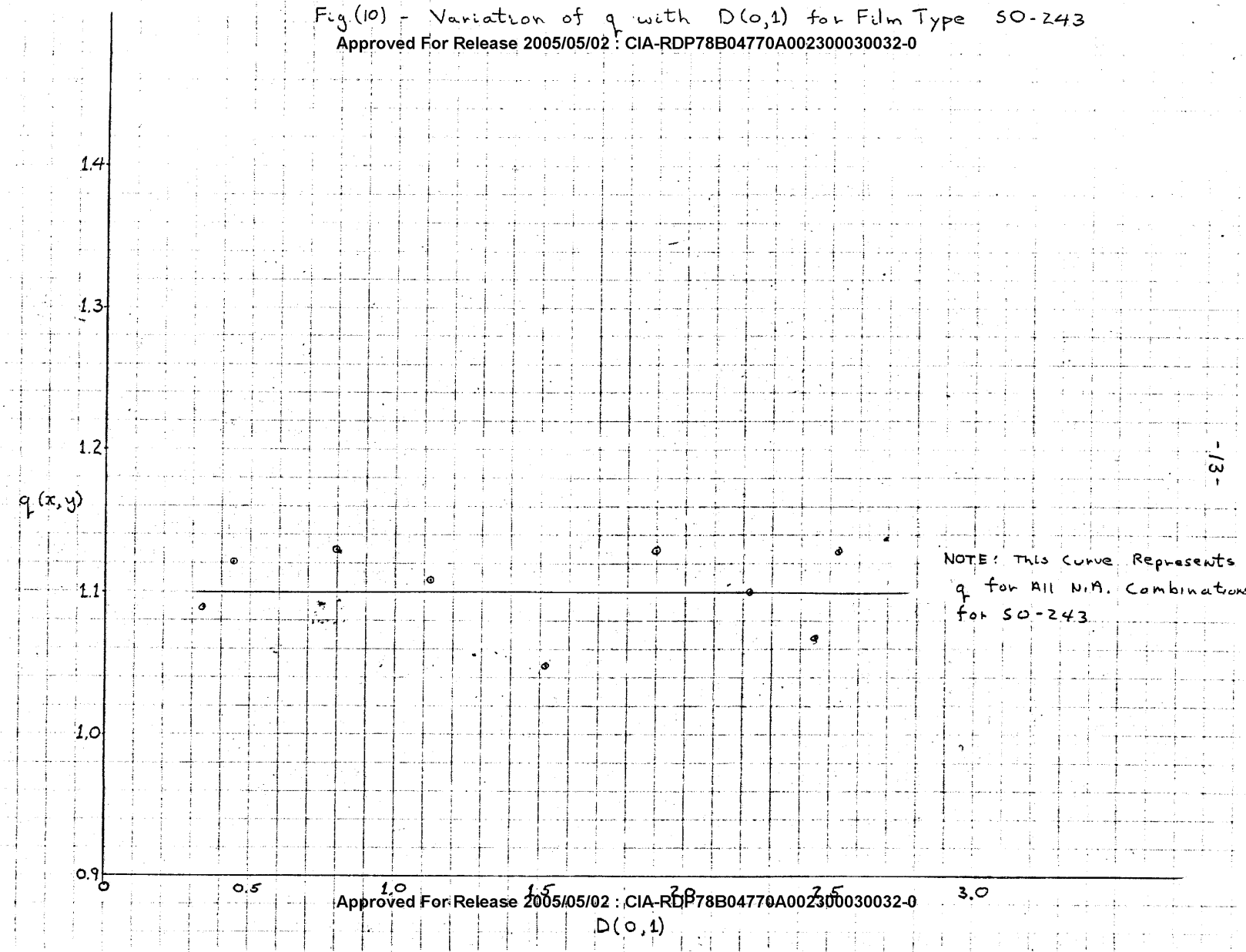

Approved For Release 2005/05/02 : CIA-RDP78B04770A002300030032-0

Fig.(11) - Variation of η with D(0,1) for Film Type SO-136 (2 min. Development)

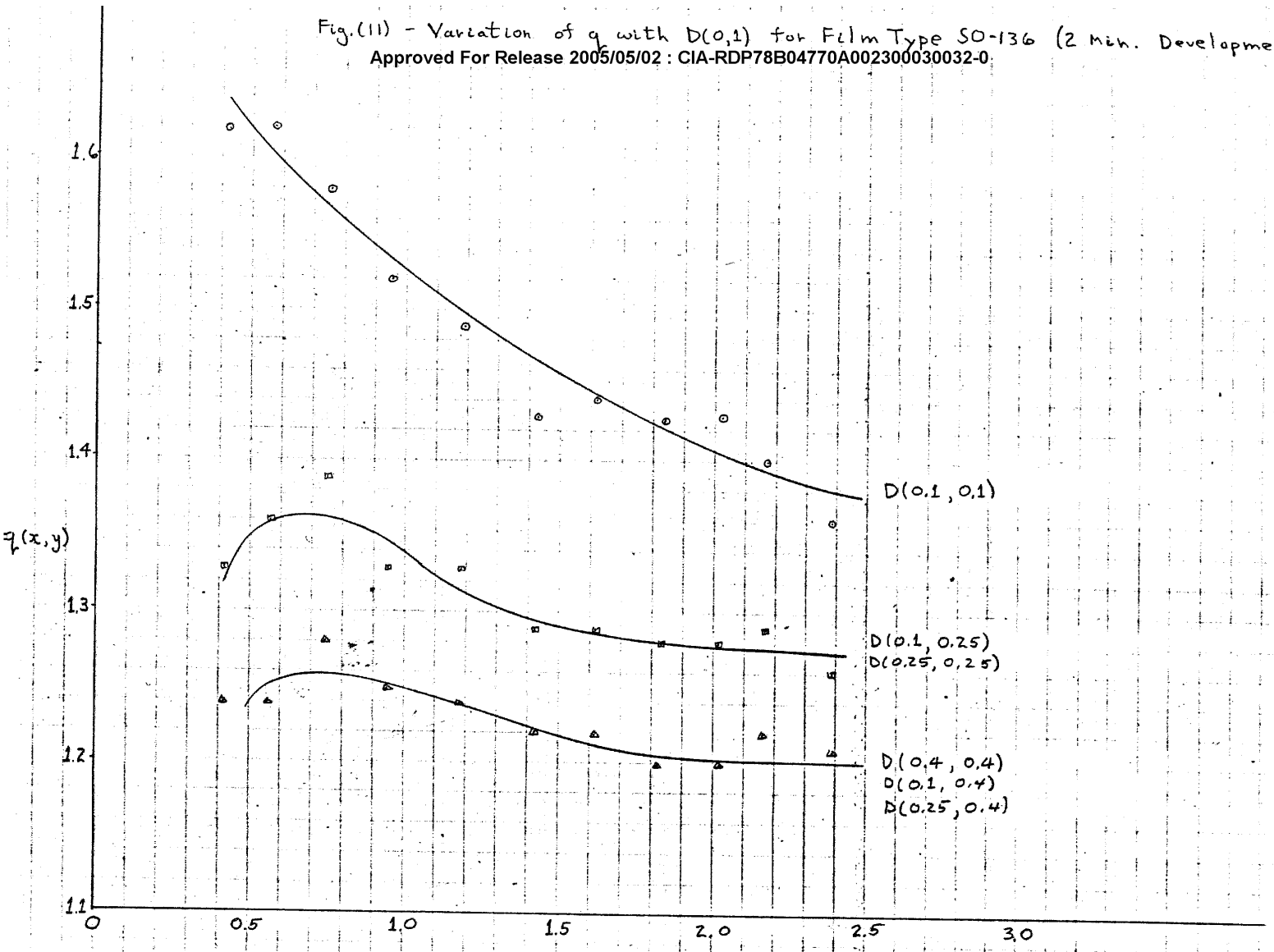

Fig. (12) Variation of q with D(0,1) for Film Type SO-136 (5 Minute Development)

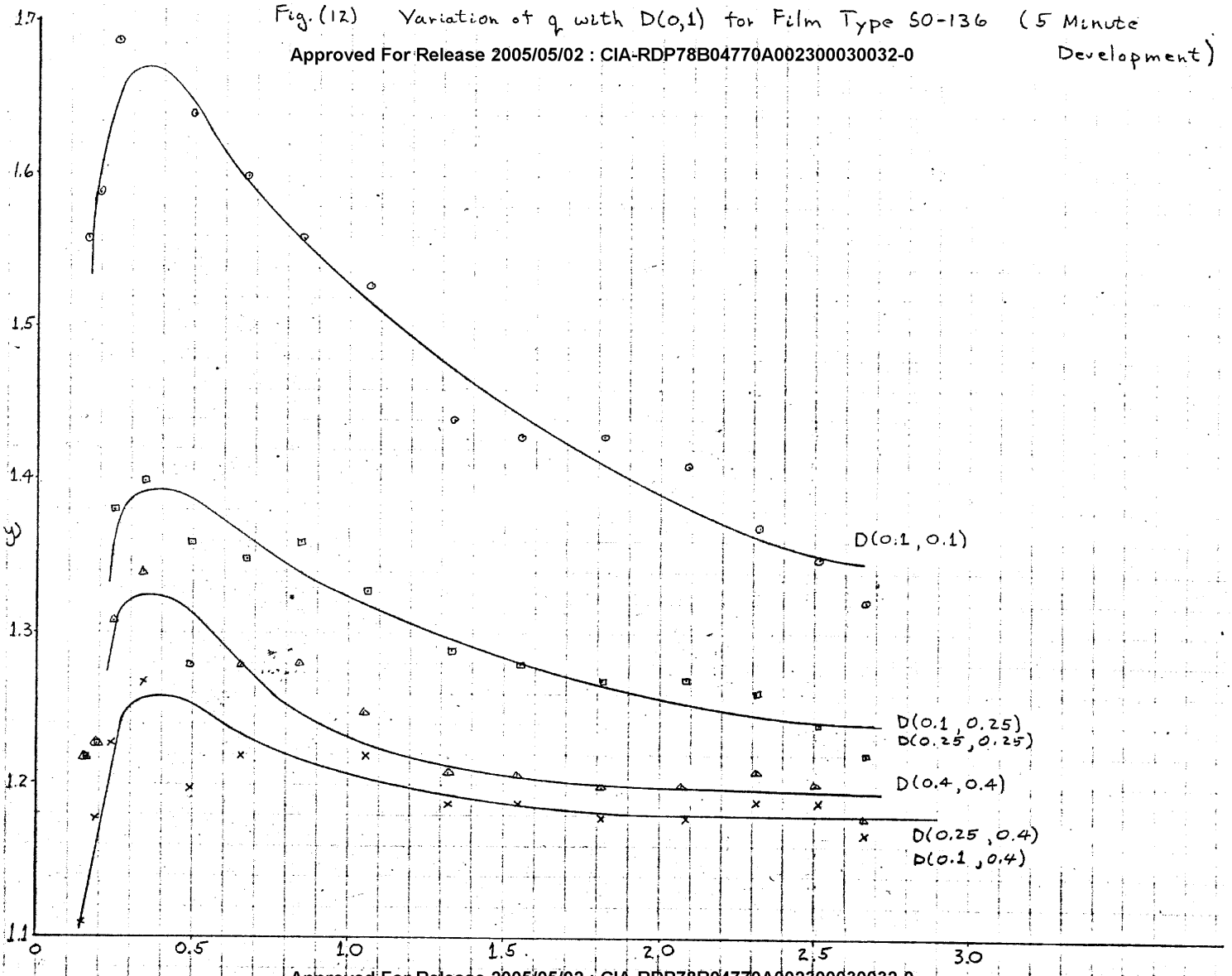

Fig.(13) - Variation of q with D(0,1) for Film Type SO-136 (12 Min. Development)

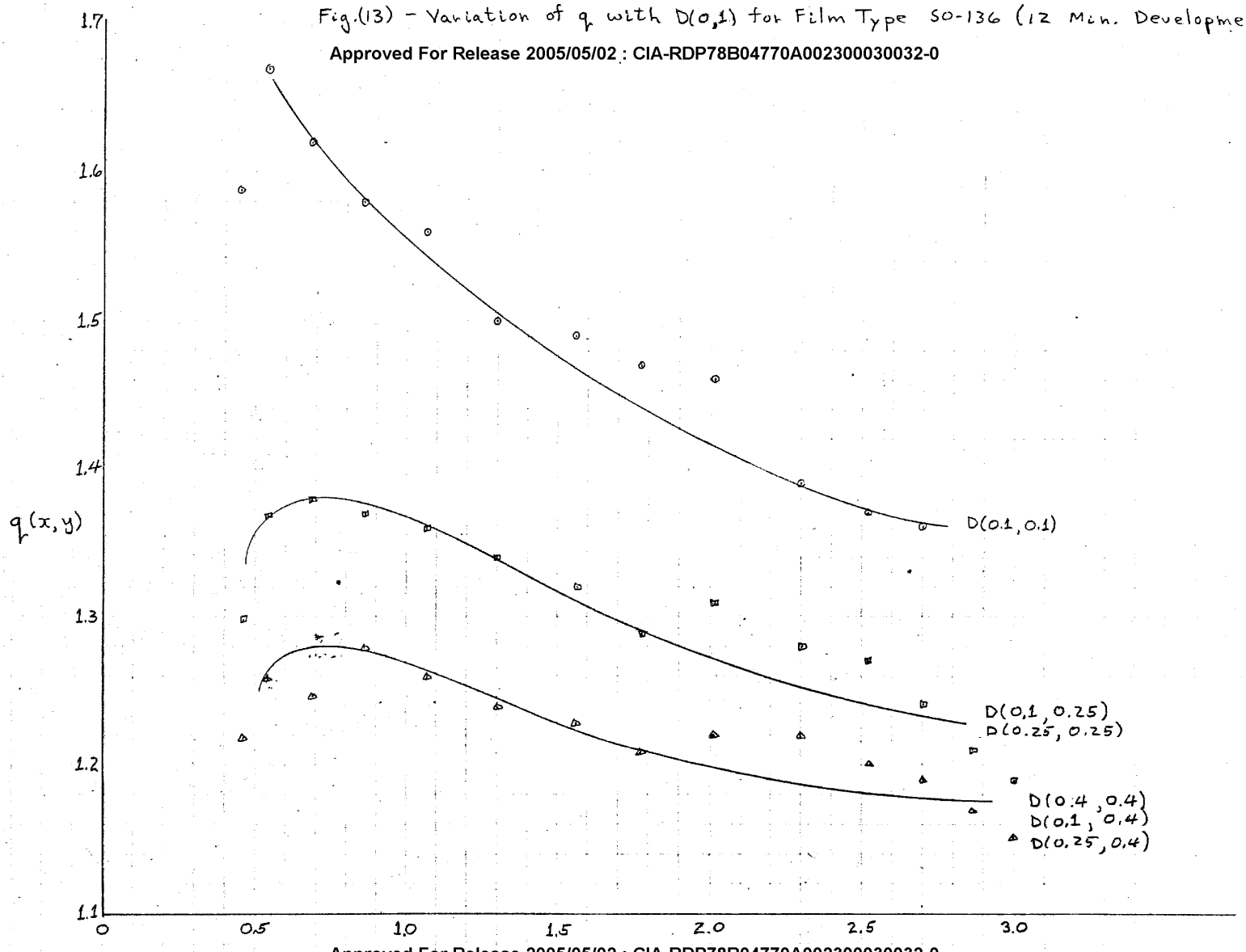

Fig.(14) Variation of q with D(0,1) for Film Type 8401

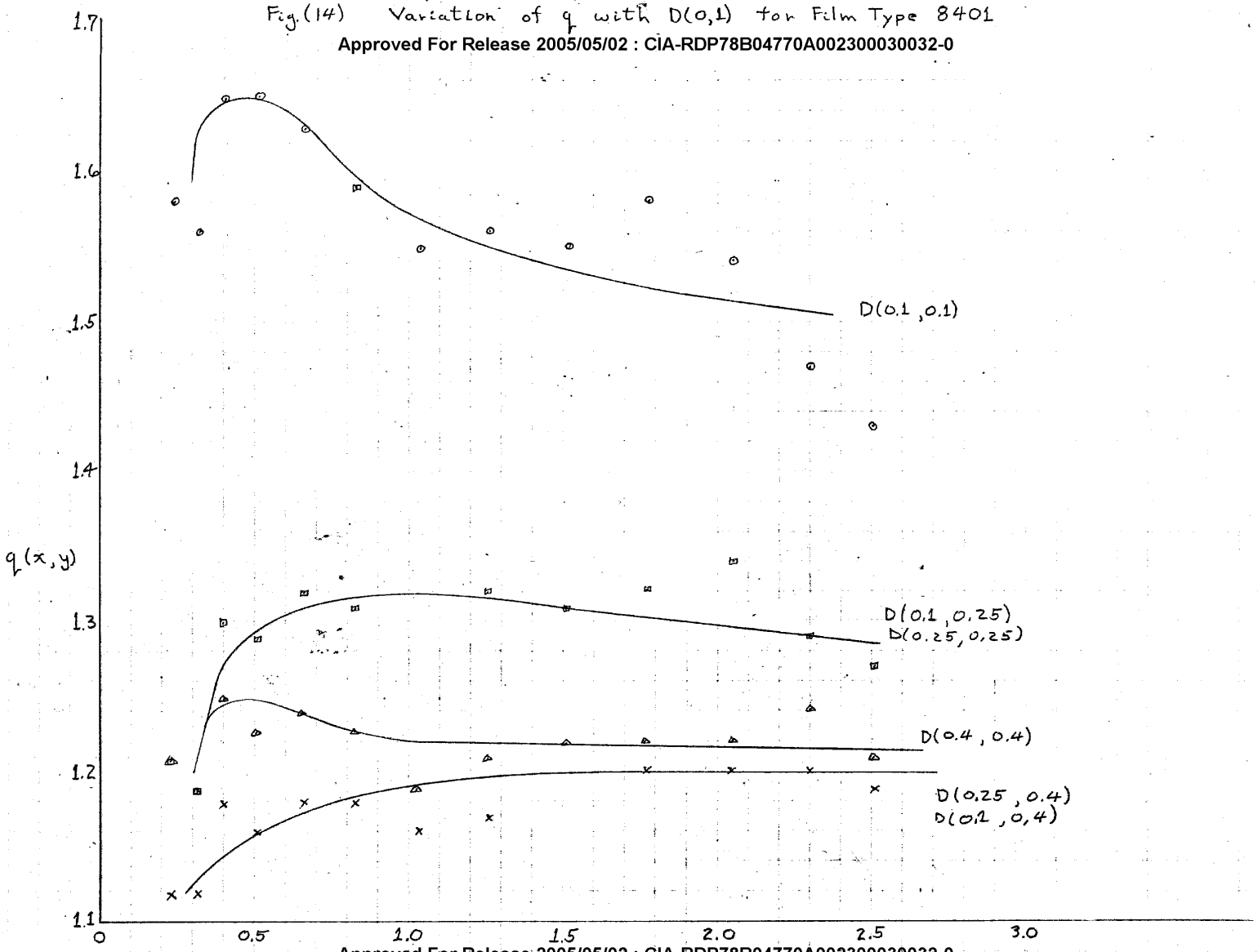

Linear Relation Between log q_r and log D(0,1)
for Panatomic-X Film

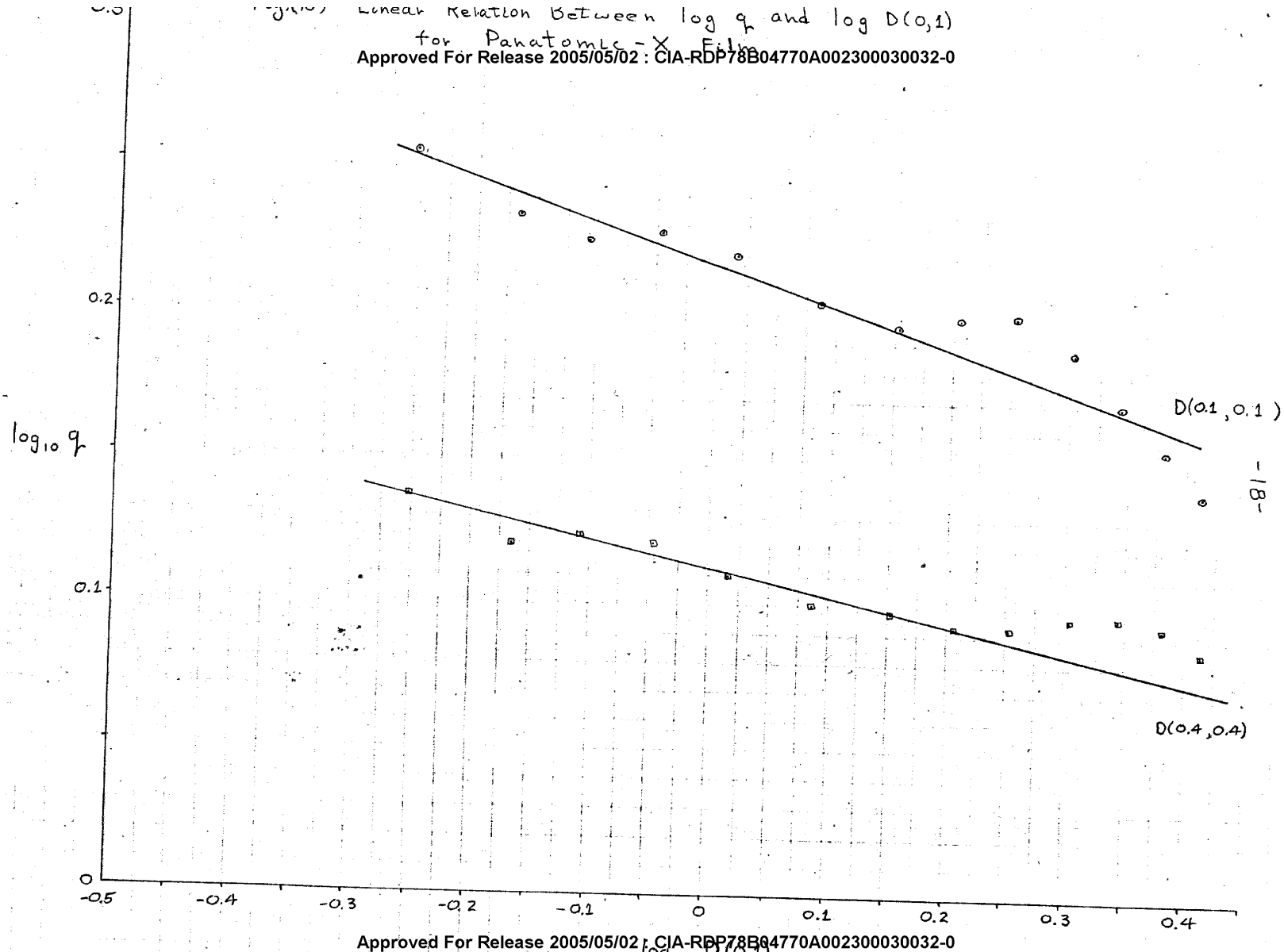

Fig (16) Linear Relation Between $\log_{10} q$ and $\log D(0,1)$ for SO-278 Film

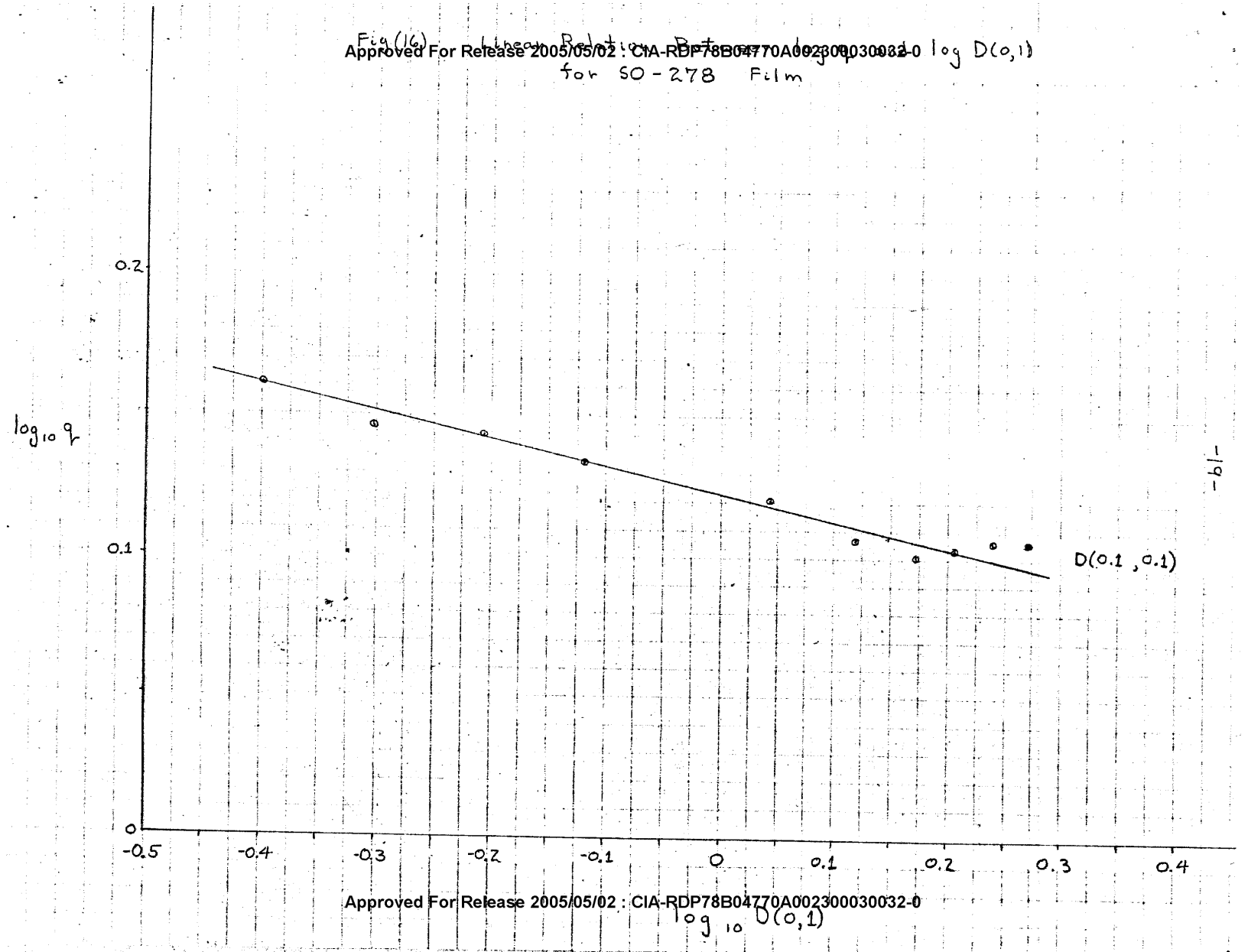

Fig. (17)- Linear Relation Between log q_r and log D(0,1)

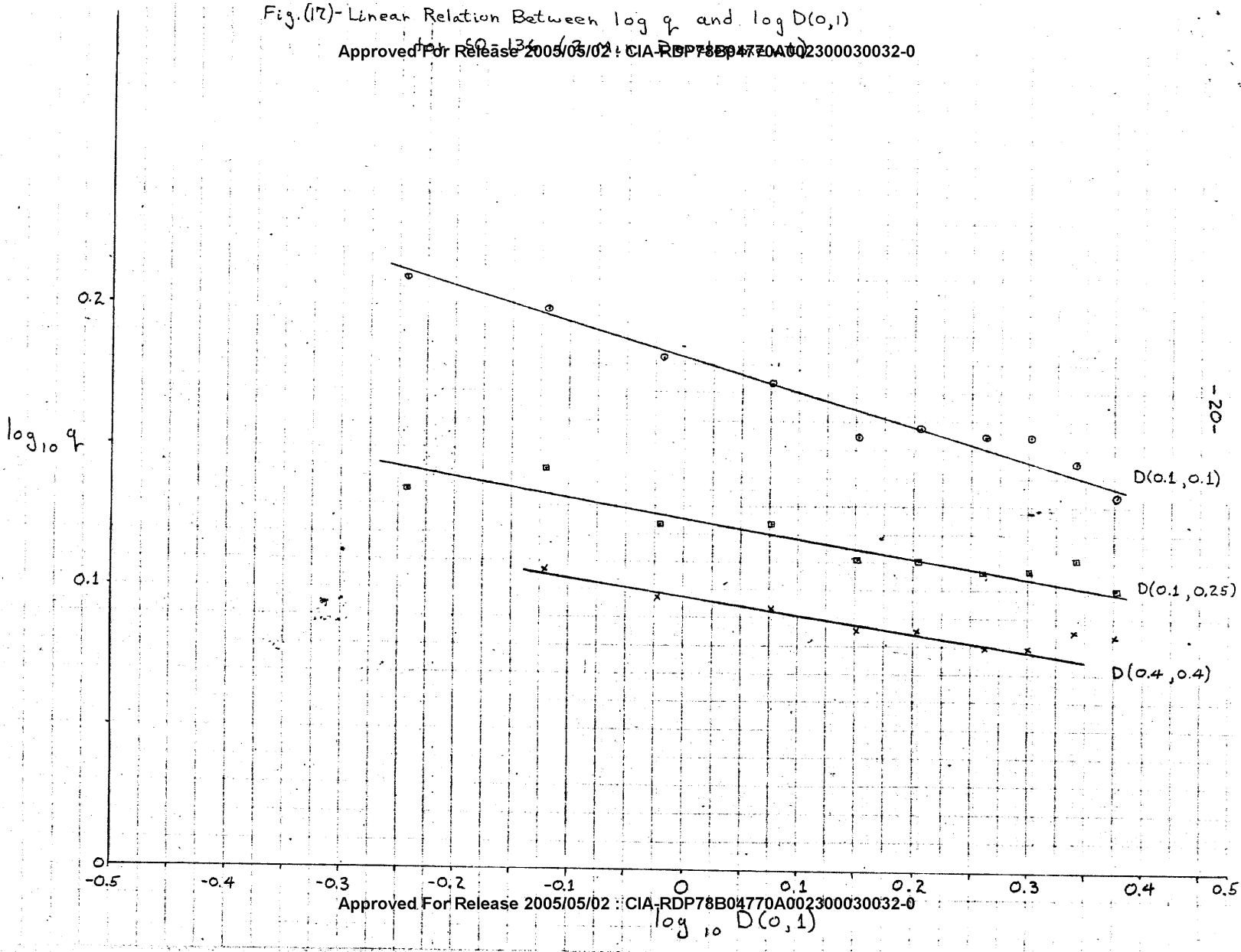

25 August 1964
MM:bb:385
(997-112)

TRIP REPORT

To: [redacted] on 6 August 1964

By: [redacted]

Purpose: To Evaluate the [redacted] Microdensitometer

Persons Contacted: [redacted]

[redacted] Attendees: [redacted]

CC:

[redacted] which handles the [redacted] line of instruments was visited on 6 August 1964 for the purpose of obtaining information concerning the [redacted] microdensitometers as part of the Project Microcap survey. The only information we had prior to the trip was an outdated (1954) [redacted] brochure.

Two basic models of microdensitometers are produced by [redacted] with the primary difference between the two being the power output of the light source.

[redacted] instrument is a double beam null type of instrument with a unique means for driving the scanning stage. The stage is directly coupled (with a rigid steel lever arm) to the chart table. The chart table is driven and the lever arm, rotating about a fulcrum point located between the chart table and the sample stage, drives the sample stage. The rate at which the tables move is controlled by a servo mechanism such that the scan speed is

inversely proportional to the rate of change of density. This is done to ensure that the recorder pen response time does not affect the result.

The location of the fulcrum point of the lever arm is adjustable to 6 different positions allowing for ratios of distance-on-the-chart-paper to distance-on-the-sample of 1:1, 5:1, 10:1, 20:1, and 50:1 (special lever arms yielding either a 100:1 and 200:1 ratio or a 1000:1 ratio are also available).

The instrument's density range is governed by a glass filter wedge which is inserted in the pen arm assembly and through which one of the beams passes. Density varies linearly along the wedge which moves until a balance is achieved between the analytic and the reference light beams. Wedges with density ranges of 0-0.5 up to 0-3.8 are available.

A major drawback of this system is that the single-scan length is limited to the chart length (11") divided by the ratio being used. The sample stage itself will accommodate film up to 10" long and the entire length can only be scanned by using a "ratchetting" technique which is time consuming and which can seriously affect the mensuration accuracy.

The set of standard tests developed for the microdensitometer evaluation study were conducted on the instrument. The 125 and the 400 cycle sine wave test patterns were not visible using the highest possible magnification and were thus not scanned. Despite the rigid coupling of the sample stage and the recording table, the mensuration precision test yielded an error greater than the reading error of the chart when the 5:1 ratio arm was used.

STAT [redacted] also handles several other types of microdensitometers including an isodensity tracer which produces a map of isodensity lines from a raster scan across a photograph and an integrating microdensitometer for use primarily in biophysics.

[redacted] STAT

25 August 1964
MM:bb:387
(997-112)

TRIP REPORT

To: on 18 August 1964

By:

Purpose: Obtain Information on the Automatic Focussing Device

Persons Contacted:

Others Attending:

CC:

and I were given a tour through new physics building where most of the photographic system performance work is done. We were shown the Model III microdensitometer which had the automatic focusing device incorporated in it and were also shown the original microdensitometer, the Model V microdensitometer, the granularity microdensitometer, the "Wiener Spectrum" microdensitometer, and the sine wave cameras used for film and lens testing.

accompanied us on the tour. The Naval Air Development Center owns a Model III microdensitometer and is interested in purchasing the automatic focusing device. was also interested in various image evaluation techniques and, from his questions, NADC is just entering the field.

The automatic focusing device (see Figure 1 for schematic diagram) was developed principally because the basic instrument would not maintain focus throughout the full length of scan available. The device will not focus on a grainless or very fine grain emulsion nor on any emulsion with high densities.

Approximately 50% of the available light is used for the automatic focusing device thus decreasing the sensitivity of the instrument. This light passes through a lens wheel which is rotating at 60 cycles per second (selected arbitrarily) and which is composed of alternate quadrants of positive and negative power. When the sample is nearly focused, the lens wheel causes the image to be alternately focused before and after an aperture which is conjugate to the microdensitometer scanning aperture. The aperture used in the automatic focusing device consists of a random array of holes. The motion of the lens wheel causes an apparent motion of the image across the random aperture giving rise to a fluctuating signal. When the analytical microscope is not quite focused on the sample, either the positive or the negative lens will focus the image closer to the random aperture which will result in a greater fluctuation in the photomultiplier dynode voltage. A servo mechanism then moves the analytical microscope until the fluctuations are a minimum which occurs when the images found by the positive and negative lenses fall equally spaced in front of and behind the random aperture. At this point the image of the sample falls on the scanning aperture.

STAT

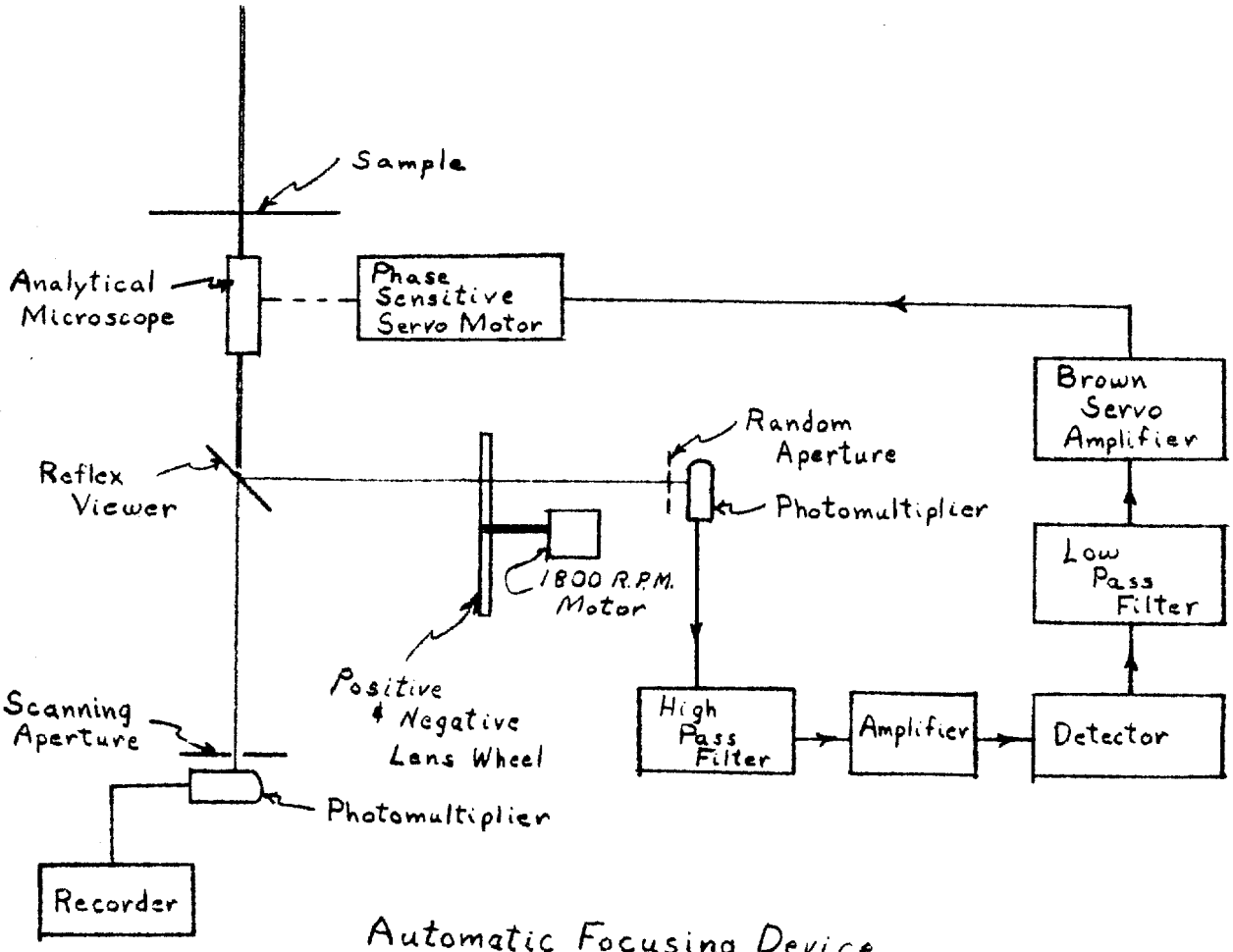

Automatic Focusing Device
(a)

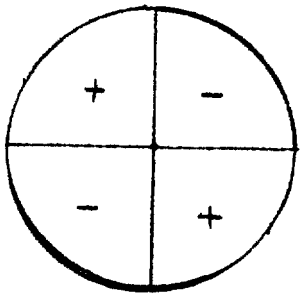

Positive-Negative Lens Wheel
(b)

Figure 1

31 August 1964
MJM:bb:400
(997-112)

TRIP REPORT

STAT To: on 20, 21 August 1964

STAT By:

STAT Persons Contacted:

STAT Other Attendee:

STAT Subject: To Evaluate the Data Microdensitometer

CC: STAT

STAT and I visited the to test their STAT microdensitometer using the tests developed for Project Microcap. Questions pertaining to various optional features available on the instrument were answered

STAT

STAT operated the microdensitometer for us since only he

STAT and use the instrument. It is located in a Whitfield type of clean room

STAT facility. was very meticulous in operating the instrument and was very well aware of the care to be taken to ensure optimum results and to preserve the mensuration capabilities of the instrument.

STAT pointed out some of the features of the instrument designed to provide accurate and stable results such as the oversized wiring and soldered terminals for the illuminating lamp. He also told us that they have noticed errors in alignment and mensuration accuracy due to the effect of body radiation.

STAT who builds the basic microdensitometer, has informed us that when making measurements accurate to one micron or less such an effect should occur.

The gas bearing film platen was also demonstrated. This device consists of an annular ring which fits around the illumination objective. Compressed gas is fed into the ring and is vented through a series of holes in the bottom of the ring. The venting gas holds the ring above the film and likewise holds the film flat against the stage. Since only a thin layer of gas is in contact with the film, it may be moved under the ring (and the objective) freely. We focused on the grain of a piece of film, pulled the film out from under the objective, moved the stage and then slipped the film back in again with no change in focus.

No details pertaining to the [redacted] Micro Spot Aperture Assembly were obtained because no patent approval has been received yet. The Micro Spot device provides an extremely small (stated as being reduced to 0.3 microns) and intense spot of light. The instrument is capable of measuring densities from about 0 to 3 with this small spot of light.

STAT [redacted] said that they had made a survey of micro comparator manufacturers and that they had found that the [redacted] was the only one who had the capability of producing a micro comparator accurate to one micron. They collaborated with the [redacted] in producing the microdensitometer now marketed by both the [redacted] and the [redacted]

STAT [redacted] has had extensive government funding to help develop a microdensitometer which they felt met their requirements. They claimed that no other instrument of this type, including Ansco's "Class I" instrument, was accurate enough. The [redacted] is currently working with NBS to develop density mensuration and resolution and linear measurement standards. They are also working with ACIC on the moon mapping program for Project Apollo.

[redacted]

31 August 1964
JS:bb:407
997-112

MEMORANDUM

STAT To:

From:

Subject: Evaluation of Microdensitometer Resolution Characteristics by Sine Wave and Edge Trace Techniques STAT

CC:

The modulation transfer function (MTF) or sine-wave response is commonly accepted as a convenient means of assessing the quality of optical systems. For this reason the approach taken for evaluating and comparing various microdensitometers was to determine the MTF of each system.

The objectives of this work are: (a) prepare and determine modulation of sine-wave test charts having frequencies of up to 800 cycles/mm, (b) prepare test edges from which the MTF of a microdensitometer can be obtained through appropriate analysis of the instrument's edge response[1] and (c) using each of the test patterns, conduct independent tests on microdensitometer to establish and STAT compare its quality characteristic as determined by the two methods.

Part I Sine-Wave Test Target Generation

A technique for generating sine-wave test charts had to be developed at STAT due to the fact that commercial charts were not available. After several techniques were attempted, the one adopted consisted of reducing a 20 lines/mm STAT square wave test pattern in the microscope reducing camera. Theoretical justification for this approach is demonstrated by first considering the uniformly convergent Fourier series representing the intensity transmittance of the square-wave pattern used as the input object.

STAT "Study of Image Quality Evaluation"
STAT Final Report, VE-1867-G-1, November 1963

$$\tau(\omega_x) = \bar{H} + \frac{4}{\pi}\left[\sin\omega_x + \frac{1}{3}\sin 3\omega_x - \frac{1}{3}\sin 5\omega_x + \cdots + \frac{1}{N}\sin N\omega_x\right] \quad (1)$$

where N is any odd integers
ω_x spatial frequency
$\bar{H}$ bias level

If all the terms following the first in Equation (1) could be eliminated, the resulting expression would be sinusoidal with frequency ω_x, and a good quality recording of the pattern on a high resolution unit gamma positive film would yield a sine-wave test chart. The elimination of these terms, when the square-wave input to the microscope camera is reduced, is achieved by the proper selection of an objective. For example, in preparing the 200 line/mm charts from the 20 line/mm square-wave input, a 10X, 0.25 N.A. metallurgical microscope objective having a diffraction limited MTF, as shown in Figure 1, was needed. Examination of Figure 1 shows that the lens transfer characteristics for imaging the 200 lines/mm image eliminates all terms above the second in Equation (1), and if the lens is carefully defocused, the MTF collapses slightly to $3\omega_x$ and the second term is eliminated with only approximately 10% loss of the fundamental modulation at the 200 cycle/mm level. This same technique was used in generating the 125 cycle chart with a 5X, 0.10 N.A. objective and the 400 cycle chart with a 20X, 40 N.A. objective.

In order for a sine-wave pattern to be a useful tool in evaluating an optical system, its modulation must be known. Determination of the modulation was done by evaluating the ratio of the diffracted to non-diffracted intensity pattern of the sine-wave grating illuminated with a gas laser of wavelength 6328 A. The expression used in computing the modulation is:

$$\text{modulation} = \left[\frac{\text{intensity diffracted}}{\text{non-diffracted intensity}}\right]^{1/2} \quad (2)$$

the derivation of which can be obtained in a [redacted] memo.[2] Evaluation of the charts STAT
using the diffraction method resulted in computed values of 59.2% for the 125 cycles, 17.6% for the 200 cycle and 24.0% for the 400 cycle chart. Attempts to get a reasonable modulation on an 800 cycle chart failed.

STAT [2] [redacted] "On the Relationship Between Sine Wave Modulation and Some Coherent Optical Filtering Measurements," ET:bb:373 (997-112), 13 August 1964

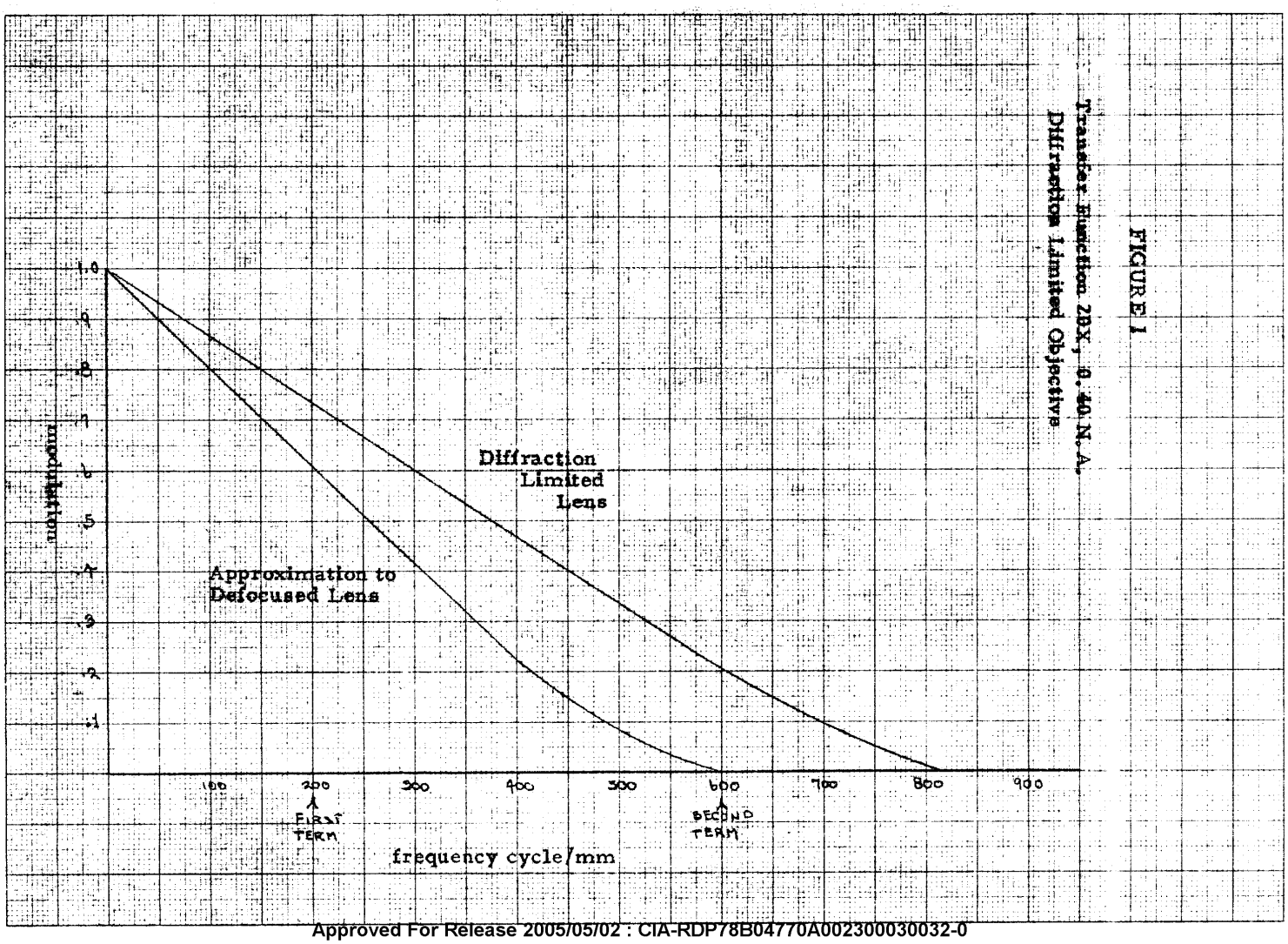

FIGURE 1

In order to verify the sinusoidal intensity transmission of each chart, two tests were conducted. The first consisted of examining the intensity distribution in the diffraction plane for the presence of unwanted harmonics. On the 125 cycle chart energy was found at 3 , but the intensity was lower than that of the fundamental by a factor of at least one hundred, whereas the 200 and 400 cycle charts were free of all unwanted harmonics, as far as could be determined by our tests (i.e., much less than 1% of the fundamental intensity).

Microddensitometer traces of each chart were made, and the intensity function of each chart was plotted against a true sine function in Figure 2. The 125 cycle plot shows a reduced and rounded peak indicating the presence of the third harmonic. Another characteristic of the 125 cycle function is skewness to the left indicating the possible presence of a second harmonic which wasn't detected in the diffraction tests because the intensity was lower than the detector sensitivity. The 200 and 400 cycle charts agree much better with the true sine function as the diffraction tests indicated they should.

Each of the three charts was scanned on [redacted] Model 4 microdensitometer. The optical combinations used in the sine wave tests and the computed sine wave response of the microdensitometer are shown in Table 1 and a discussion of the results is given in Part III of this memo. STAT

Microdensitometer Optical System			Microdensitometer Response		
Eyepiece	Objective	Effective Aperture	100 Cycles	200 Cycles	400 Cycles
12.5X	10X	2.0 μ x 152 μ	50%	32.5%	4.7%
12.5X	20X	1.0 μ x 76 μ	62.7	72.5	28
12.5X	40X	0.5 μ x 38 μ	62.7	72.5	23

TABLE 1

Microdensitometer Optical Systems and Responses
for Sine Wave Tests

Part II Edge Evaluation

By converting density to exposure and differentiating the edge response of a microdensitometer, the line spread function of the system is obtained. The mathematical Fourier transform of this function can then be taken and the response

FIGURE 2
(Page 1)

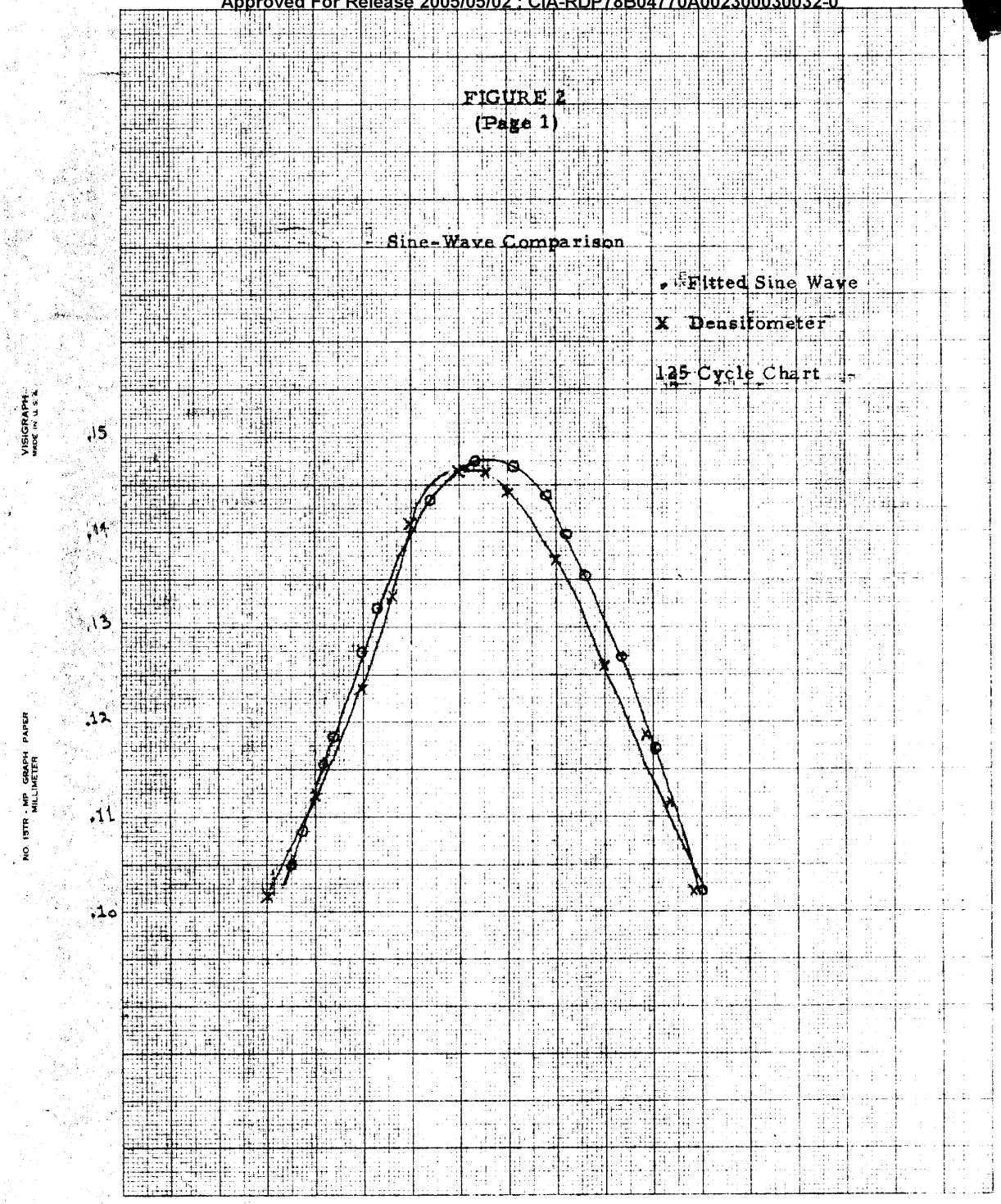

FIGURE 2
(Page 2)

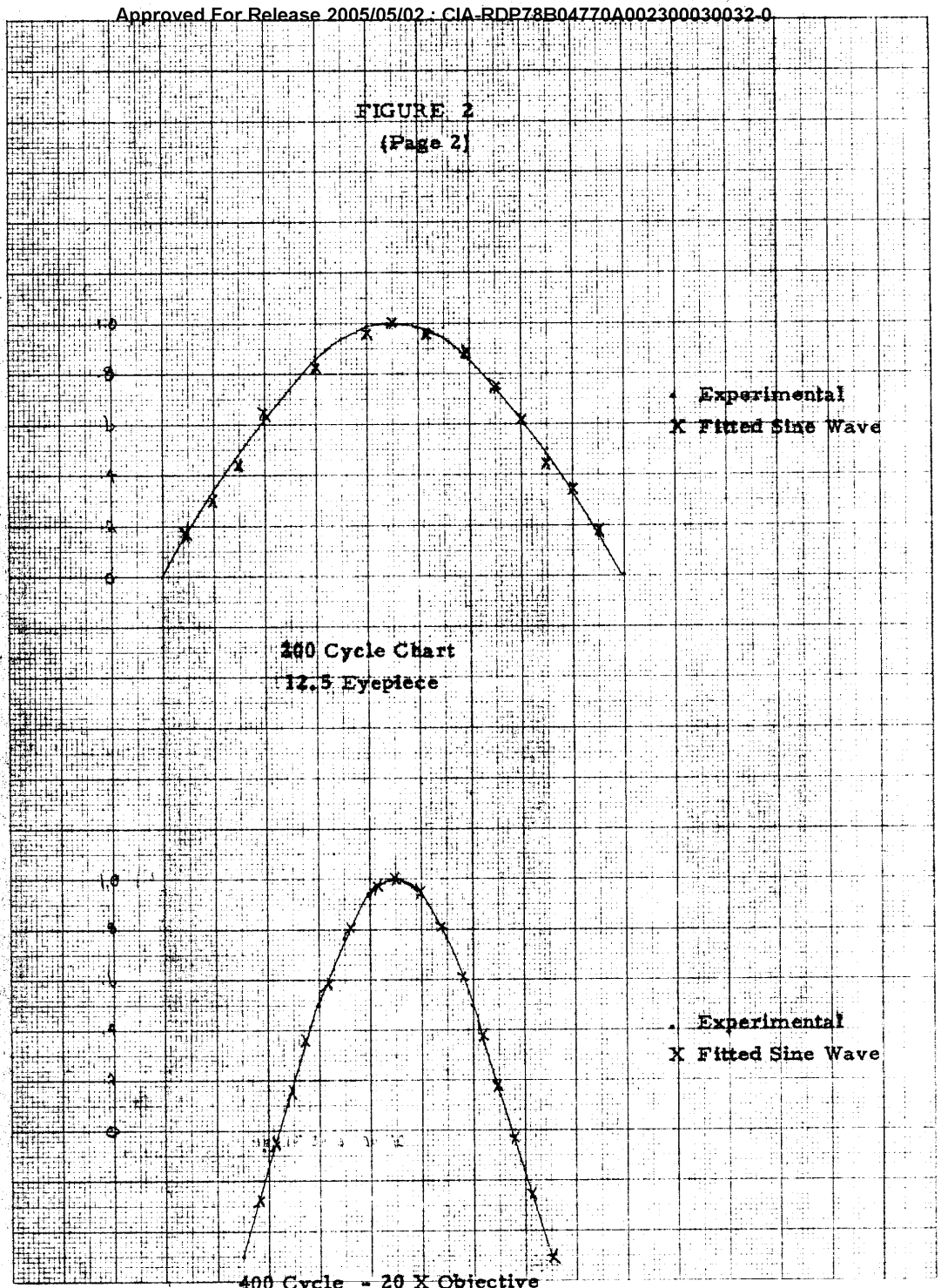

400 Cycle - 20 X Objective
12.5 X Eyepiece

of the system (MTF) obtained. The problem involved is obtaining an edge response which is limited by the optics and not by the edge. For a microdensitometer system which perhaps may be capable of 1000 lines/mm this means the edge quality must be at least twice that of the system limit or 2000 lines/mm resulting in an acceptable edge width no greater than 0.5 μ .

Preparation of an edge to be used in the edge evaluation was done in the following manner. A single edge razor blade was first honed to eliminate its saw-toothed edge (easily seen with 20X magnification) and then mounted in the object plane of the [redacted] diffraction limited microscope reducing camera. A 40X, 0.65 N.A. microscope objective having a resolution capability in excess of 2000 lines/mm was used to image the razor edge on Eastman high resolution SO-105 microfilm. Following the normal development of the image, a post-development chemical treatment of the edge image in a sub-proportional density reducer was used for additional sharpening of the edge.[3] The mechanism of this post treatment involves bleaching the lower densities at a greater rate than the higher densities resulting in (1) elimination of randomly developed grains on the clear side of edge and (2) increasing the slope of the density transition.

STAT

Edge traces were obtained with the [redacted] microdensitometer using the range of microscope objectives available with a 12.5X eyepiece and constant physical aperture. Table 2 gives the optical combinations used in the edge tests.

STAT

Eyepiece	Objective	Effective Aperture
12.5X	5X	4.0 μ x 304 μ
12.5X	10X	2.0 μ x 152 μ
12.5X	20X	1.0 μ x 76 μ
12.5X	40X	0.5 μ x 38 μ

TABLE 2

Microdensitometer Optical Systems Used for Edge Tests

Modulation transfer functions computed on [redacted] IBM 704 computer are shown for each scan in Figure 3.

STAT

[3] C.E. Mees, "The Theory of the Photographic Process," Revised Edition, McMillan 1954, pp. 738-740

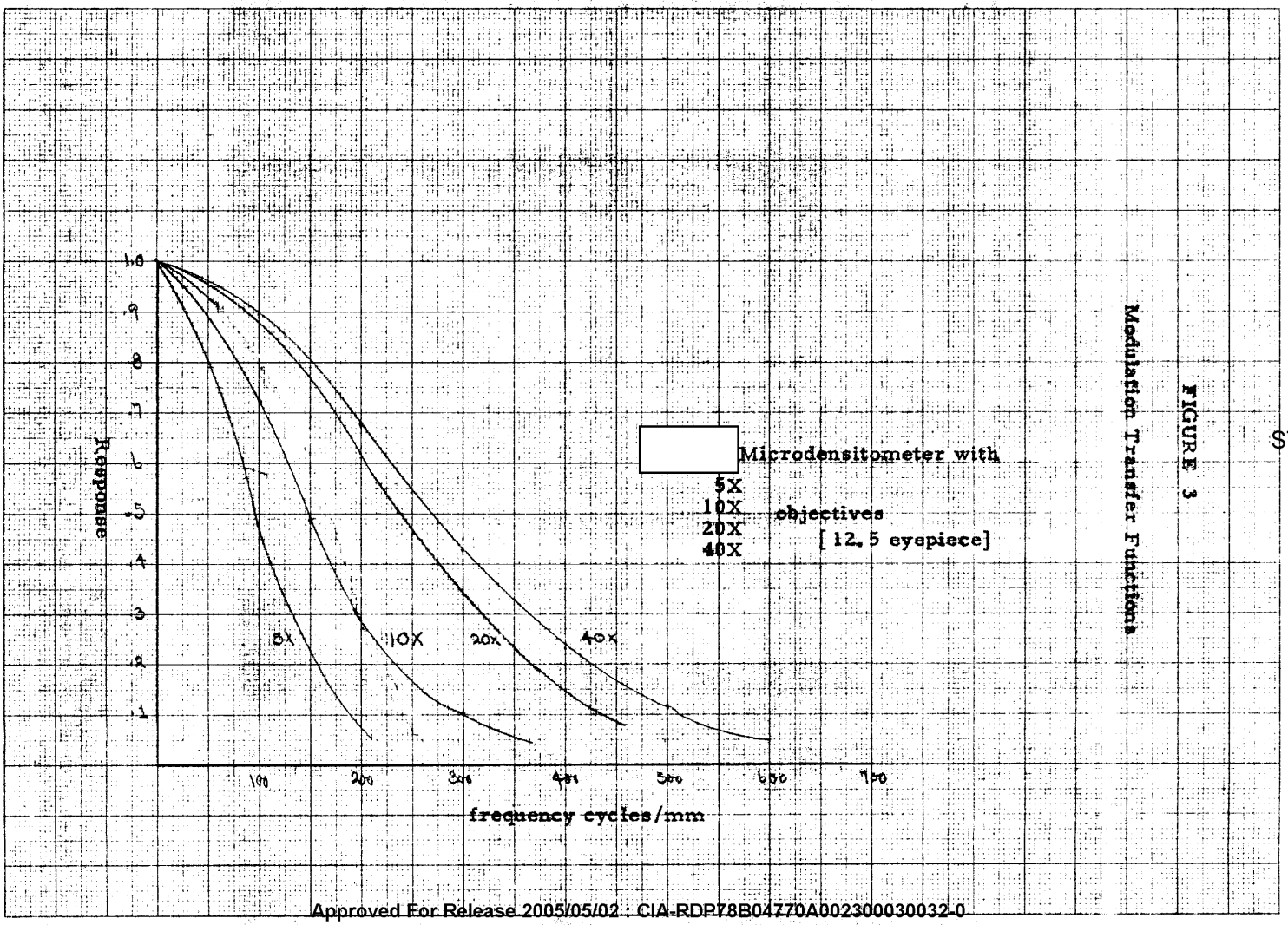

FIGURE 3

Modulation Transfer Functions

STAT

Part III Results and Evaluation of the Tests

It was expected that the modulation values for the edge trace and sine-wave scan procedure would agree giving us verification of our results by two independent tests. The results of both tests are plotted on Figure 4. It can be seen that reasonable agreement exists at the 200 and 400 cycle/mm frequencies. However, at the 125 cycle/mm frequency the values obtained from the sine-wave test are in all three cases approximately 17% lower than those from the edge tests.

This 17% difference at the 125 cycle/mm frequency can be explained by the existence of the third harmonic in the 125 cycle chart which was too small to be determined accurately. This being the case, generation of harmonic-free charts is not possible without modification of the present technique or employing a new method.

STAT

STAT

FIGURE 4

Modulation Transfer Functions

From [redacted] Microdensitometer

1) Data points sine-wave test values

2) Curves are from edge evaluation